Setting Environmental Limits

STATISTICAL ASPECTS OF TURBIDITY MONITORING

Limitations Statement

The sole purpose of this document is to identify options for the statistical analysis of turbidity data as provided to Environmetrics Australia Pty. Ltd. by the Port of Melbourne Corporation (PoMC). The analyses and techniques presented herein are intended to be indicative only. The passage of time, manifestation of latent conditions or impact of future events may require further exploration, subsequent data analysis, and re-evaluation of the findings, observations, conclusions, and recommendations expressed in this document. Accordingly, Environmetrics Australia Pty. Ltd. accepts no liability or responsibility whatsoever for or in respect of any use of or reliance upon this document, its recommendations or any other information contained herein by any party.

STATISTICAL ASPECTS OF TURBIDITY MONITORING:

SETTING ENVIRONMENTAL LIMITS

Prepared for Port of Melbourne Corporation

By

Environmetrics Australia Pty. Ltd.

April 2007

Table of Contents

List of Figures

1. INTRODUCTION

This report summarises work associated with the establishment of 'appropriate' environmental limits for turbidity during the proposed dredging operations in Port Phillip Bay. Specifically, it addresses the following key questions that formed part of PoMC's brief to Environmetrics Australia:

- What NTU would deliver 15% of surface irradiance at 3m depth for a minimum of 50% of the time during dredging?;
- What NTU would deliver 15% of surface irradiance at 3m depth for a minimum of 50% of the time during the most intense 2 week period of dredging?

Our companion report "Statistical Aspects of Turbidity Monitoring: Control Charting" discusses cost-effective turbidity monitoring strategies that attempt to balance rates of 'false-triggering' with the need for an 'early-warning' capability. It must be kept in mind that both reports are concerned only with the statistical issues associated with setting and monitoring environmental limits. It is recognised that the ultimate numerical limits and the monitoring protocols adopted will consider a much broader set of issues that integrate not only the statistical aspects of risk, but social, economic, and political dimensions as well. Thus the numerical 'limits' or triggers identified in this report should be regarded as a starting point – they have been developed using sound statistical theory and methods, but do not in themselves represent the complete picture.

There are a number of components to the evaluation of a benthic light climate that might prevail before, during, and after dredging operations. Those that are most relevant to the impacts of dredging have been identified in Figure 1 together with the various physical and inferential processes involved.
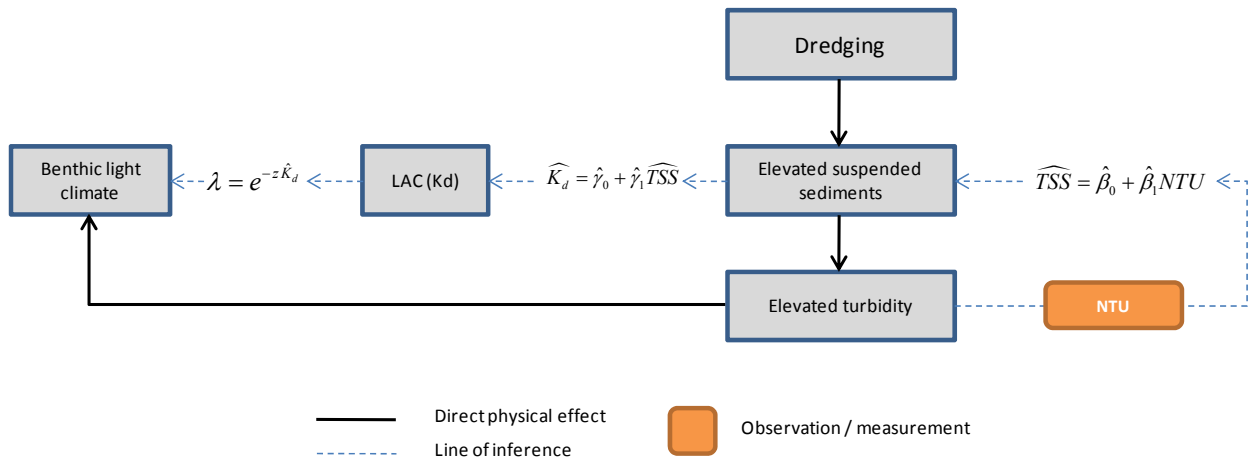
Figure 1. Key physical processes and inferential steps associated with an evaluation of benthic light climate. (LAC – light attenuation coefficient).

Figure 1 shows a highly simplified version of the physical processes involved in the assessment of benthic light climate and it is recognised that this is not complete – for example re-suspension and settling of sediments is not considered and uniform mixing through the water column is assumed. Nevertheless it is considered adequate for the purpose of statistical modelling with a view to addressing the key questions listed above. It is clear that one of the direct effects of dredging is to mobilise sediments which in turn will lead to an increased concentration of suspended particulate matter in the water column. This increased sediment concentration manifests itself as cloudiness or turbidity. The elevated turbidity reduces the amount of light passing through the water column. Although the quantum of light reaching some depth z (metres) can be measured directly, this is not practical for a large-scale dredging operation. It is far more convenient to collect data on a (surrogate) measure of turbidity and to use these data to *infer* the light climate at some depth, z since *TSS* cannot be measured directly or in real-time. There are a number of measures of turbidity, although one of the more common is Nephelometric Turbidity Units (NTU) which is determined by measuring the scattering of light as it passes through the liquid. The broken lines in Figure 1 show the various stages in the inferential process. From Figure 1 we note that three regression models are involved in the final determination of the benthic light climate. The first model converts a *measured* NTU into a predicted *TSS* (total suspended sediment concentration). A comprehensive investigation into the nature of this relationship can be found in the report *"An*

Examination of Regression Options for TSS and NTU" (Environmetrics Australia 2007a). The final form of the relationship established in that report was:

$$TSS_i = 1.4462\, NTU_i + \varepsilon_i \tag{1}$$

where ε_i is a random error term assumed to be normally distributed with zero mean and variance σ_ε^2.

The amount of light reaching depth z metres is expressed by the relationship

$$\frac{I_Z}{I_0} = \exp\left(-z\, K_d\right) \tag{2}$$

where I_0 and I_Z are the amounts of light at the surface and at depth z respectively and K_d is the light attenuation coefficient (LAC). The quantity $\frac{I_Z}{I_0}$ is thus the *fraction* of the surface irradiance measured at depth z and is denoted by λ in Figure 1. Baker et al. (1984) showed that theoretical calculations of attenuation based on scattering by spherical particles underestimated observed attenuation by factors of 2-4. This is apparently because physical irregularities of natural particles give them a larger optical diameter than that of a theoretical sphere of equal volume. It has also been observed that the LAC is not constant but varies with changing sediment concentration. The relationship between *TSS* and K_d is modelled as:

$$Kd_i = \gamma_0 + \gamma_1 TSS_i + \xi_i \tag{3}$$

where ξ_i is a random error term assumed to be normally distributed with zero mean and variance σ_ξ^2. The analysis of field and laboratory data in Appendix A yielded the following parameter estimates: $\hat{\gamma}_0 = 0.29587$ and $\hat{\gamma}_1 = 0.023757$. The intercept of approximately 0.3 is reflective of the mean attenuation coefficient over the Bay in the absence of dredging impacts (see Appendix A).

A critical aspect of Figure 1 and equations 1 and 3 is that of *uncertainty*: each of the models given by equations 1 and 3 has associated with it a level of error which will manifest itself as uncertainty in values predicted from the corresponding model.

To further complicate matters is the issue of 'cascading uncertainty' – that is, the uncertainty in a *TSS* predicted from an *NTU* reading (call it NTU_0) will propagate through the inferential chain identified in Figure 1. Thus, the predicted *TSS* (call it $\widehat{TSS_0}$) can be expressed as the sum of the *true* (but unknown) TSS_0 and an error, ε_0 whose exact value is also unknown. This predicted *TSS* becomes an *input* at the next stage – that is, the predicted K_d is based on a *predicted TSS*. Given that the relationship between *TSS* and K_d is itself imprecise, we have a situation of compounding uncertainty. This is not an uncommon situation in modelling physical systems, although a full and adequate treatment of the *total* error or uncertainty is often overlooked or neglected. It is only by quantifying the uncertainties associated with each of the equations 1 and 3 and following those through the chain of calculations can a meaningful assessment of the overall uncertainty in the quantity of interest (λ) be made. Furthermore, as a result of these uncertainties, statements concerning a predicted λ require either a companion statement of *precision* or alternatively need to be couched in terms of probabilities. We have chosen the latter and this report specifically focuses on a *probabilistic* assessment of benthic light climate under various dredging scenarios.

2. A PROBABILISTIC ANALYSIS OF BENTHIC LIGHT CLIMATE

The various steps associated with simulating benthic light climate data are illustrated in Figure 2. The process commences with a probability model for *NTU* – this can be either the total *NTU* (background + contribution due to dredging as predicted from hydrodynamic models) or just background *NTU* if an analysis of conditions without dredging is required.
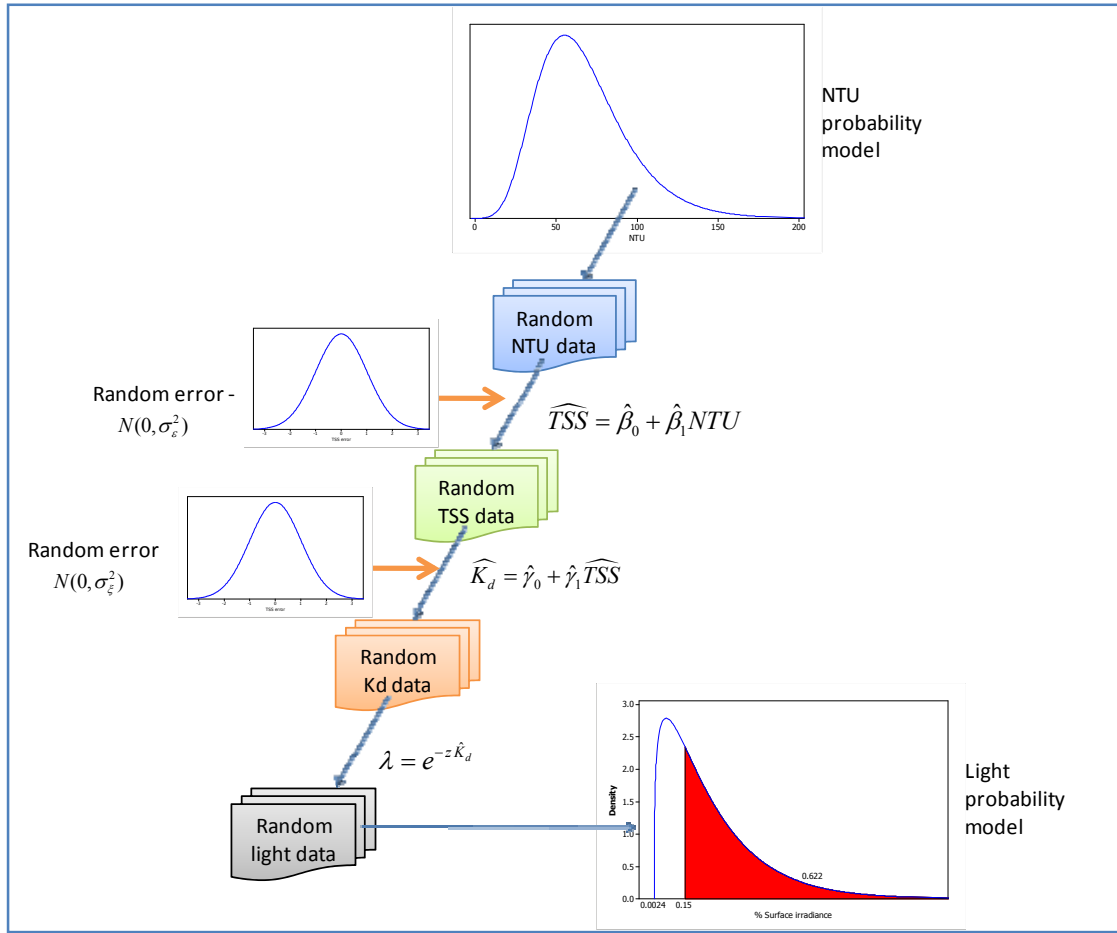
Figure 2. Schematic of process used to make a probabilistic assessment of benthic light climate.

An *NTU* observation is randomly generated from the *NTU* probability model and using equation 1, the conditional mean of the *TSS* distribution at this particular *NTU* is determined. A separate calculation (see Appendix B) provides an estimate of the variance of this *TSS* distribution. This conditional *TSS* distribution is then used to randomly generate a single *TSS* observation. A value of K_d is then randomly generated from a distribution conditioned on the previously generated *TSS* value. Finally, equation 2 is used to obtain a value of λ and the process is repeated. Note, that these steps: (i) honour the 'true' distribution of *NTU* values expected in the natural environment; (ii) preserve the relationship between *TSS* and *NTU*; (iii) introduce the appropriate level of uncertainty in a predicted *TSS* *conditioned* on the 'observed' *NTU* and (iv) acknowledge and account for the uncertainty in the $K_d - TSS$ relationship. By repeating this process many times (the results in this report are typically based on 100,000 simulated values) we can use the empirical distribution of λ (the fraction of surface irradiance reaching the seafloor) to assess the likelihood

that a 15% light requirement, say, is met (ie. $\lambda \geq 15\%$). We believe that this approach provides a comprehensive and realistic assessment of turbidity-induced light climate impacts. Results of these analyses are presented in the following two sub-sections. The first set of results relate to overall or 'average' conditions during the dredging campaign. The second set of results focus on a 'worst fortnight' scenario. All results are for site 2006 in the southern portion of the Bay as this site has been identified by the Project proponents as being at greatest risk (with respect to turbidity impacts on seagrass).

2.1 Setting an environmental limit for turbidity at site 2006: 'average' conditions

In accordance with the process shown in Figure 2, the first step involves generating *NTU* data from a suitable probability model. Computer modelling associated with the proposed dredging operations undertaken by PoMC consultants has provided estimates of the *additional* increase in suspended sediments at a number of sites in the Bay[1]. *TSS* data extracted from the model for site 2006 was converted to *NTU* values and added to the *observed* (background) *NTU* data collected by PoMC at Cameron's Bight. This was done on a 30-minute time step for the period 9-Feb-2005 to 3-Dec-2005 by matching the day/month/hour/minute of modelled *NTU* (disregarding year) with day/month/hour/minute of observed *NTU*. Due to incomplete or missing *NTU* data, a total of 9,630 *NTU* observations were generated by this process. The empirical *cdf* for the *logarithm* of these data is shown in Figure 3.

---

[1] The following advice was received from PoMC: "Dredging in the South of the Bay will be delivered in blocks. An indicative dredging schedule has been prepared for the SEES. However it is recognized that the actual dredging schedule will be delivered in accordance with the SEES. Therefore, for conservatism, the modeled TSS results should be considered as if the dredging is delivered in a single campaign".
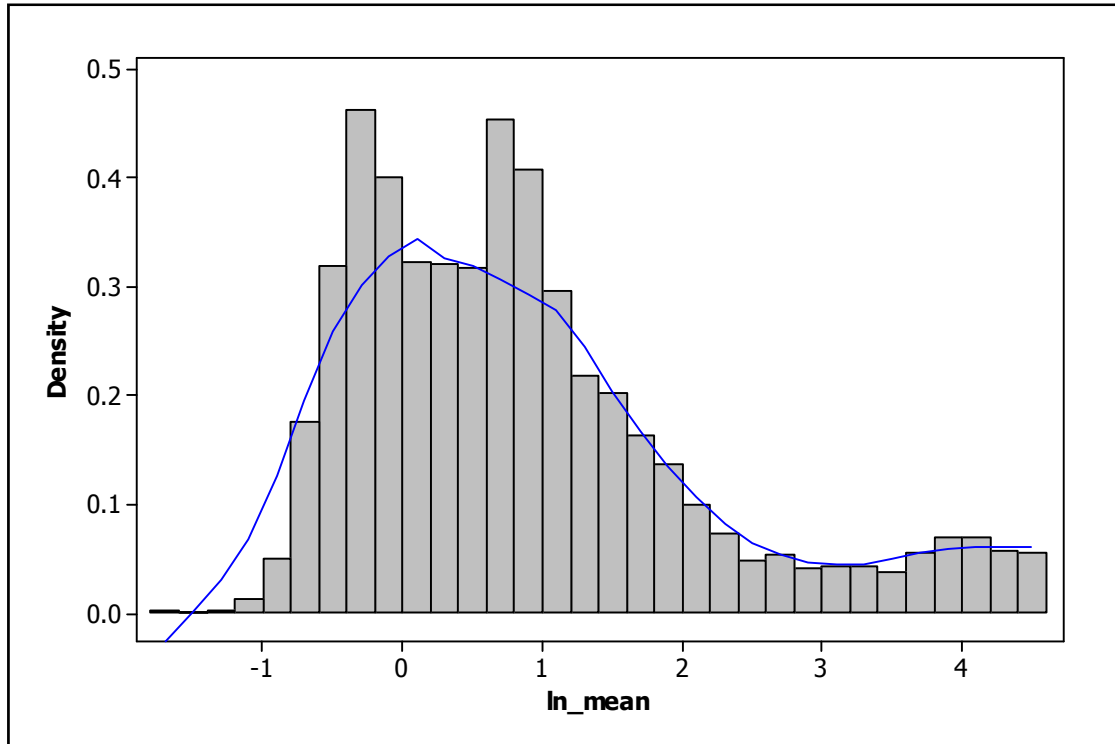

Figure 3. Empirical histogram with smoother (blue line) for *ln_total* (model + background) *NTU* at site 2006.

Figure 3 suggests that the overall *NTU* distribution is potentially a mixture of two or three distributions. This is not unreasonable and is possibly reflective of seasonal effects as well as the contributions to *NTU* from different sources, namely background and dredging. Additional analysis of these data suggested that the histogram of Figure 3 is well described by a mixture of three normal distributions. The parameters of these distributions and the mixing ratios are given in Table 1. Using these parameter values the theoretical distribution can be constructed (Figure 4). The *NTU* distribution of Figure 4 captures the features of the empirical distribution exhibited in Figure 3. As a further check on the adequacy of this description of the empirical data, the *cdf* of 50,000 values generated from the theoretical model was compared with the empirical *cdf* (Figure 5). The two distributions in Figure 5 are almost indistinguishable over the range 0 – 250 *NTU*. Table 2 provides various numerical summaries for both distributions.

Table 1. Parameters for 3-component probability model for ln(NTU).

mean	Standard deviation	Mixing parameter
0.1546096	0.5781415	0.612
1.446796	0.07081465	0.301
3.846313	0.04941749	0.087
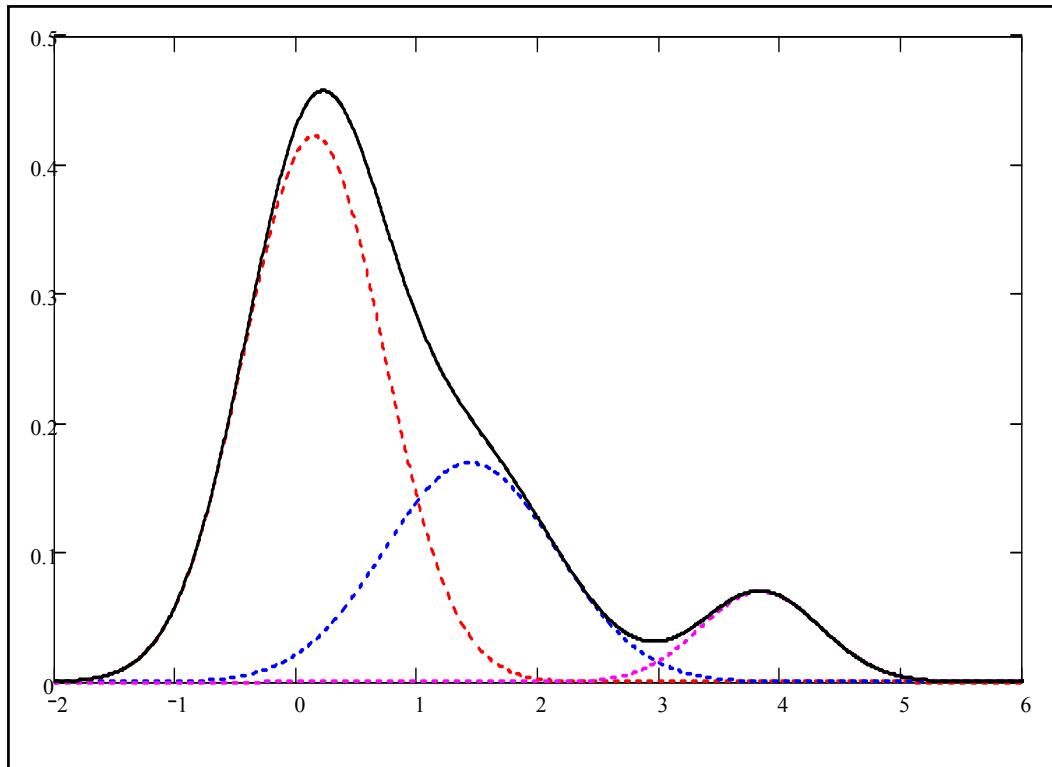
Figure 4. Mixture of three normal densities for *ln_total* (model + background) *NTU*.

It can be seen from Table 2 that the descriptive statistics for both distributions are also in close agreement, although the observed maximums are substantially different. This is due to the censoring of the empirical data which is a device limitation[2].

---

[2] The devices used in acquiring the data used in this report truncated readings at 96 NTU.
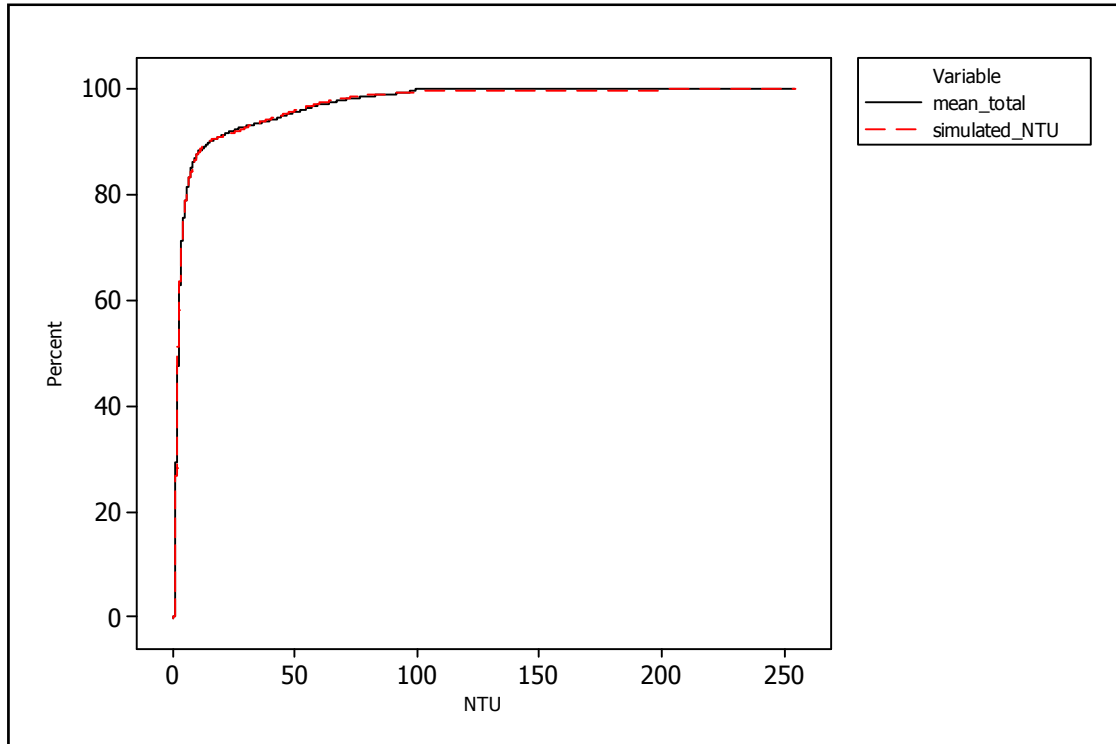
Figure 5. Comparison of empirical *cdf* for total *NTU* (solid black line) and *cdf* for simulated data (broken red line).

Table 2. Descriptive Statistics: empirical and simulated_NTU

Variable	N	N*	Mean	SE Mean	StDev	Minimum	Q1	Median	Q3	Maximum
Empirical NTU	3940	0	6.979	0.250	15.709	0.169	0.915	1.926	4.019	99.475
simulated_NTU	10000	0	6.991	0.163	16.257	0.112	0.981	1.761	4.050	254.182

A computer simulation model corresponding to the 'system' depicted in Figure 2 was developed and run using the WinBugs software (MRC Biostatistics Unit, Cambridge, UK). A program listing appears in Box 1.

Results

The computer simulation was run 100,000 times with data collected on various model outputs. A graphical summary is provided in Figure 6.

Box 1: WinBugs simulation program

```
model;
{

T ~ dcat(P[])                 #  T is a vector of mixing proportions for 3-component
normal
y~dnorm(m[T],tau[T])     #  y is a randomly generated ln(NTU) from 3-component
normal.
R11<-exp(y)                   # R11 is a randomly generated NTU with dredging

 R2 ~ dlnorm(0.002179,1.426)

# R2 is a randomly generated NTU without dredging (uncorrected for threshold
parameter)

 R3<-R2+0.0002079            # R3 is R2 corrected for threshold
mu11<-1.4462*R11          #  mu11 is mean TSS corresponding to generated NTU
(with dredging)
t11<-1/(a1*pow(R11,2))        # t11 is precision associated with predicted TSS
(with dredging)

mu12<-1.4462*R3           #  mu12 is mean TSS corresponding to generated NTU
(without dredging)
t12<-1/(a1*pow(R3,2))             # t12 is precision associated with predicted TSS
(without dredging)

TSS1 ~ dnorm( mu11,t11)I(0,400)  # TSS1 is randomly generated TSS (with
dredging)
TSS2 ~ dnorm( mu12,t12)I(0,400)  # TSS2 is randomly generated TSS (without
dredging)

mu21<-0.29587+0.023757*TSS1      # mu21 is mean Kd corresponding to generated
TSS (with dredging)
t21<-1/(s2+a2+2*b2*TSS1+c2*pow(TSS1,2))

# t21 is precision of Kd corresponding to generated TSS (with dredging)

mu22<-0.29587+0.023757*TSS2      # mu22 is mean Kd corresponding to generated
TSS (without dredging)
t22<-1/(s2+a2+2*b2*TSS2+c2*pow(TSS2,2)) # t22 is precision of Kd corresponding
to generated TSS (without dredging)

KD1 ~ dnorm( mu21,t21)     # KD1 is randomly generated Kd (with dredging)
KD2 ~ dnorm( mu22,t22)     # KD2 is randomly generated Kd (without dredging)

par1<-exp(-3*KD1)          # par1 is % surface irradiance @3m (with dredging)
par2<-exp(-3*KD2)          # par1 is % surface irradiance @3m (without dredging)


ind11<-equals(max(par1,0.15),par1)      # ind11 is indicator variable = 1 if
par1>15%; =0 otherwise (with dredging)
ind12<-equals(max(par2,0.15),par2)      # ind12 is indicator variable = 1 if
par2>15%; =0 otherwise (without dredging)

ind21<-equals(max(KD1,1.0),KD1)  # ind21 is indicator variable = 1 if Kd>1; =0
otherwise (with dredging)
ind22<-equals(max(KD2,1.0),KD2)  # ind22 is indicator variable = 1 if Kd>1; =0
otherwise (without dredging)


}

list(a1=0.00362367,a2=0.002307,b2=-0.00006339,c2=0.000004588,s2=0.165879)
list(P=c(0.6122896,0.3010061,0.0867043),m=c(0.1546096,1.446796,3.846313),tau=c(2
.99179,1.9941314,4.094856))
```
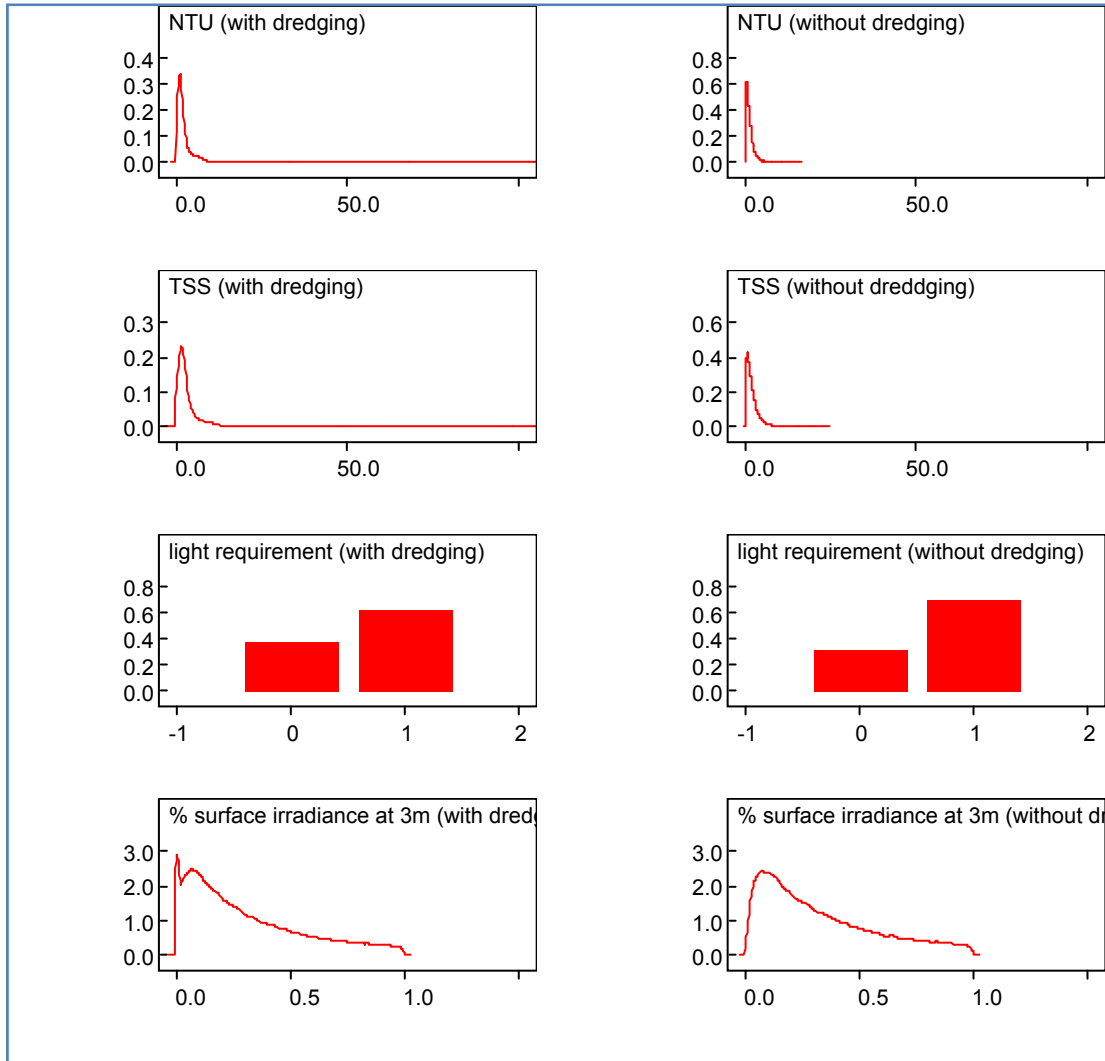
Figure 6. Histograms of various model outputs for 100,000 runs of simulation model. Note: binary outcomes for light requirement histograms are coded as 0=not met; 1=met.

An analysis of the simulation output suggests that the minimum 15% benthic light requirement (at 3m depth) will be met 62% of the time during dredging (over the entire dredging period). In the absence of dredging this 15% light requirement is met about 70% of the time at this site. During the dredging period the average *NTU* will increase from a background of around 1.5 units to 6.7 units corresponding to an increase in the average *TSS* concentration from 2.2 mg/L to 9.6 mg/L.

It is important to note that the additional turbidity from dredging at site 2006 as predicted by hydrodynamic modelling is, on average quite small (Figure 7).
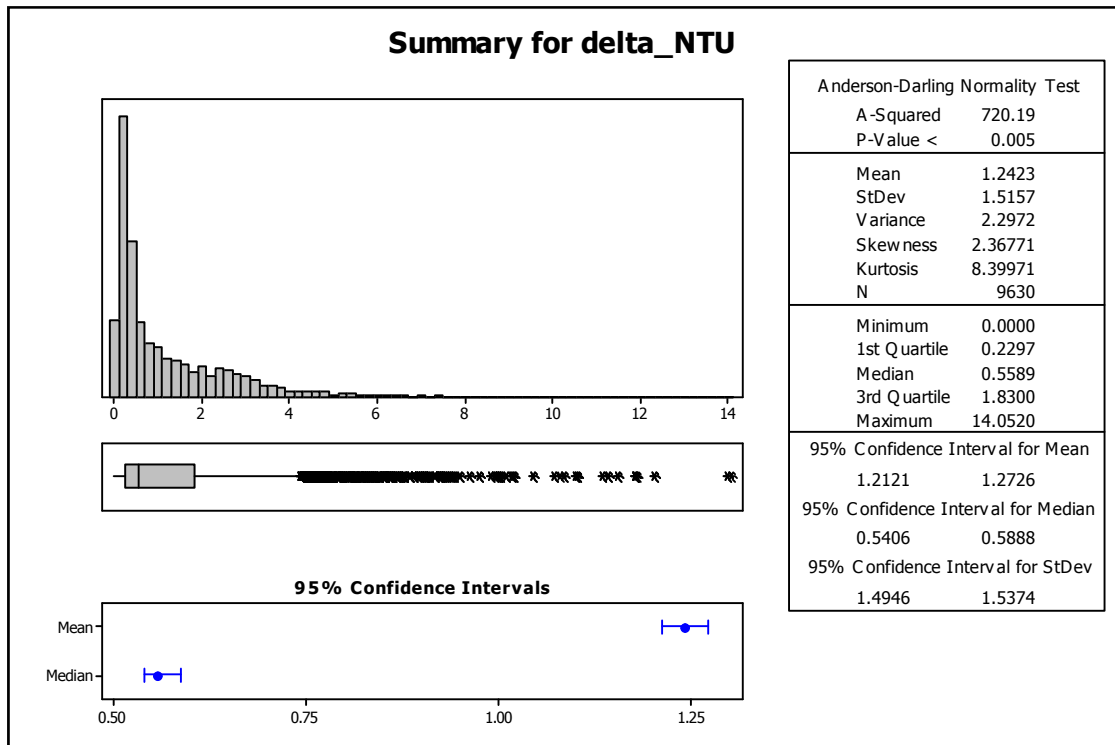
Figure 7. Statistical summary for modelled incremental *NTU* at site 2006 due to dredging.

An examination of background turbidity levels at Cameron's Bight during the months in 2005 that align with the months during which dredging is expected to take place shows that, at times the background turbidity levels are relatively high (Figure 8). From Figure 8 we see that background turbidity peaked at 96.6 although most are below 2. The implications of these observations are that the environmental assets in the vicinity of site 2006 are periodically experiencing high 'natural' turbidity (presumably associated with CDOM[3], algal pigments etc.).

---

[3] Coloured dissolved organic material
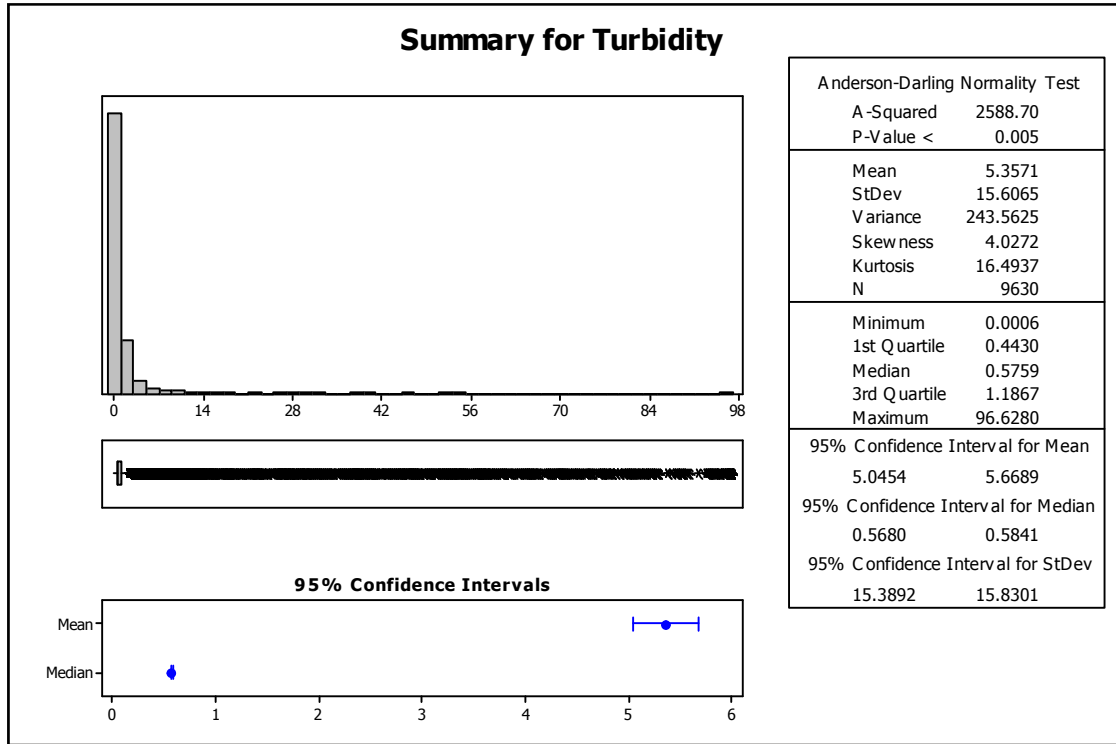
Figure 8. Statistical summary of ½ hourly background turbidity levels at Cameron's Bight Feb - Dec 2005.

Significance of the results

Providing the background and modelled data are both accurate and representative of expected conditions at site 2006, the requirement that the light at 3m depth being at least 15% of surface irradiance for more than 50% of the time (overall the entire dredging period) is expected to be met. Thus, in this context, intervention aimed at limiting peak *NTU* levels is not required since the light criterion is expected to be satisfied *over the duration of the dredging campaign*. This is not to say that there will not be instances of highly elevated turbidity which may result in periods of a substantially degraded light environment. This issue is investigated in the next section.

2.2 Setting an environmental limit for turbidity at site 2006: 'worst-case' conditions

The minimum light criterion has been expressed in terms of a minimum percentage of surface irradiance reaching depth z metres. For the present exercise, the minimum at 3m depth is taken to be 15%. A time dimension was subsequently introduced leading to the more precise requirement that the minimum 15% surface irradiance should be maintained at depth 3m *for at least 50% of the time*. While this is a more specific target, the issue concerning the time-frame to which the '50% of the time' requirement applies was not addressed. Thus, while the results of the preceding section indicate that the 15% light requirement would be met for at least 50% of the time <u>over a 10 month period</u>, this result says nothing about the likelihood that the criterion will be satisfied on shorter time-scales. The situation is depicted in Figure 9. Figure 9a shows 30 time units; half of which are light and half are dark. In this case, 50% of the total time is classified as 'light'. Figure 9b shows a different permutation of the same 30 time units arranged into 6 blocks each of 5 units. A zero or one indicates whether or not the block contains at least 50% light units. This criterion is satisfied for only 2 of the 6 blocks, ie. 33% of the time blocks.

(a)

(b)
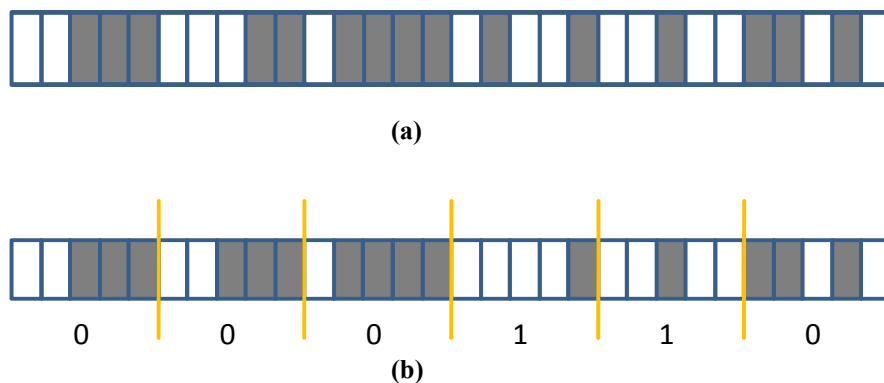
Figure 9. Two arrangements of 'light' and 'dark' time units; minimum light requirement is satisfied in (a) but not in (b).

Thus, the critical issue is the identification of the shortest period of time such that failure to meet the minimum light requirement over this time period would result in an adverse outcome. This is *not* a statistical issue and as such is not addressed by this

report. There is apparently no generally accepted minimum time period over which a minimum light requirement must be maintained to ensure seagrasses health. However, for the purpose of this evaluation, this has been taken to be a two week period.

Results

'Rolling' two week blocks formed from the combined (modelled + background) *NTU* data for site 2006 were examined to identify the 'worst' two week period (Figure 10)[4]. Examination of all blocks of 14 days for which mean *NTU* exceeded a nominal value of 6 revealed that there were 101 such 14-day blocks. An analysis of these 101 blocks identified the two week period 6-Nov (05) to 20-Nov (05) as the 'worst' fortnight.
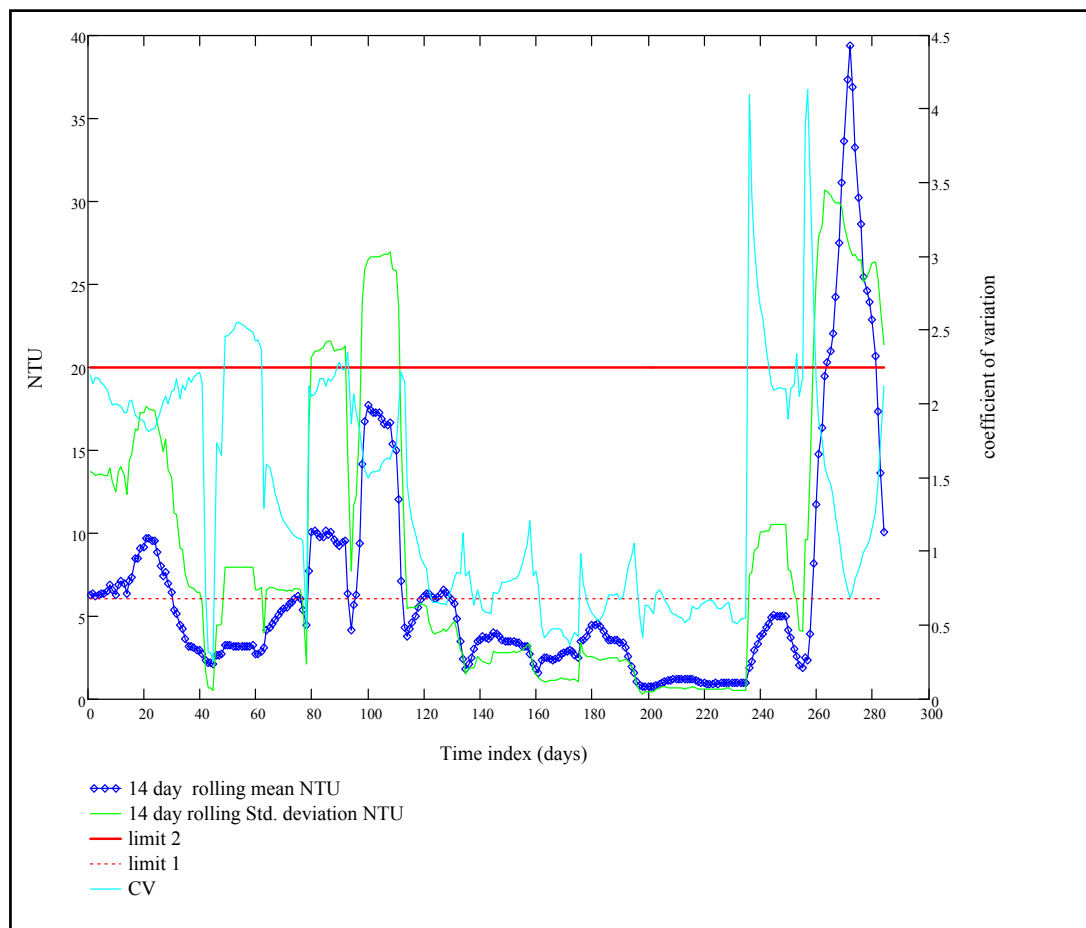

Figure 10. Time series plot of mean 14-day NTU; standard deviation of 14-day *NTU*; coefficient of variation at site 2006.

---

[4] Note: the 14-day blocks were formed by stepping a window of width 14days over the entire series. This resulted in 284 such blocks.

During this period the mean (median) *NTU* was 39.95 (40.31). The minimum was 1.10 and the maximum was 96.82.

The empirical and fitted distribution functions for *NTU* during this two week period are shown in Figure 11.

Empirical CDF of NTU
3-Parameter Lognormal

Loc	4.420
Scale	0.3188
Thresh	-48.01
N	224
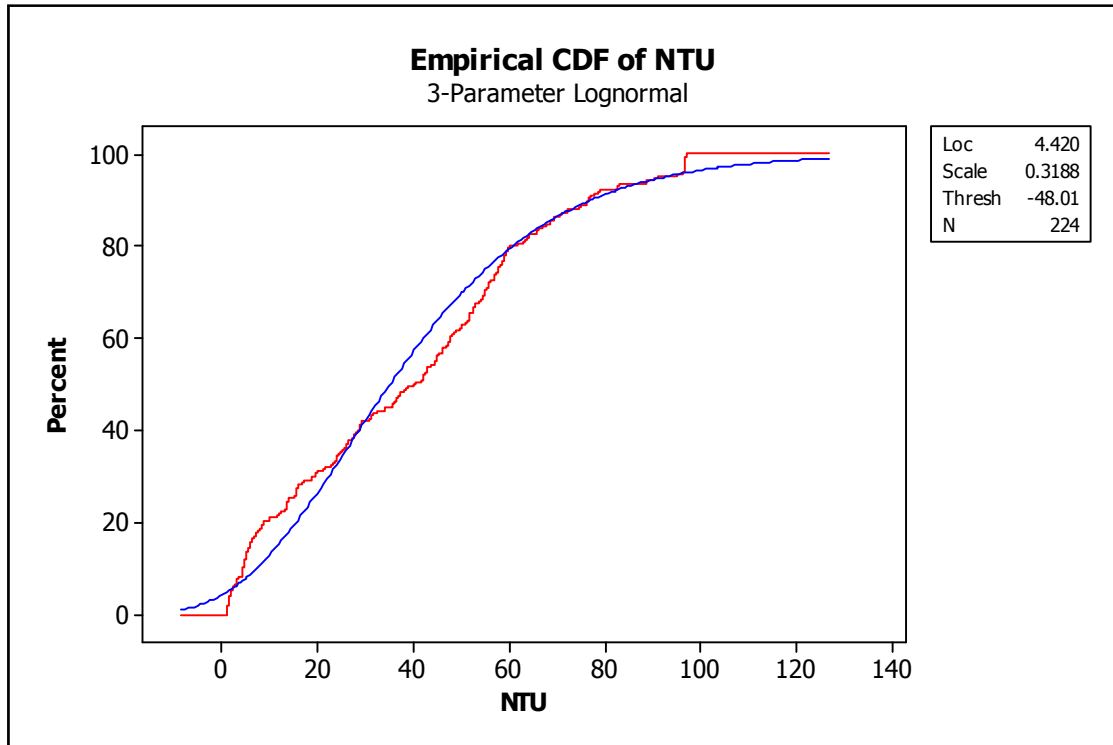
Figure 11. Fitted (blue curve) and empirical distribution functions for total *NTU* at site 2006 betweeen Nov 4 and Nov 20, 2005. Parameter estimates given in top-right box are for the log-normal *pdf*.

The three-parameter lognormal distribution of Figure 11 was used to randomly generate *NTU* data corresponding to the 'worst' 2-week period and the simulation approach described in section 2.1 was used to obtain data on the proportion of time that the 15% light requirement at 3m depth was met. An examination of the 100,000 simulated λ values indicated that the 15% light requirement would only be met 10% of the time during this 'worst-case' two-week period. During this 'worst' two week period the <u>average</u> *NTU* (*TSS*) could be as high as 66 (96) with a maximum in excess of 180 (260).

By plotting the empirical probability of successfully maintaining the 15% light requirement as a function of *NTU* (Figure 12) a 'trigger' or cut-off can be determined. Thus, we see from Figure 12, that in order to maintain the 15% light requirement at 3m depth for at least 50% of the time during this 'worst-case' fortnight, the *NTU* needs to be kept below 15.
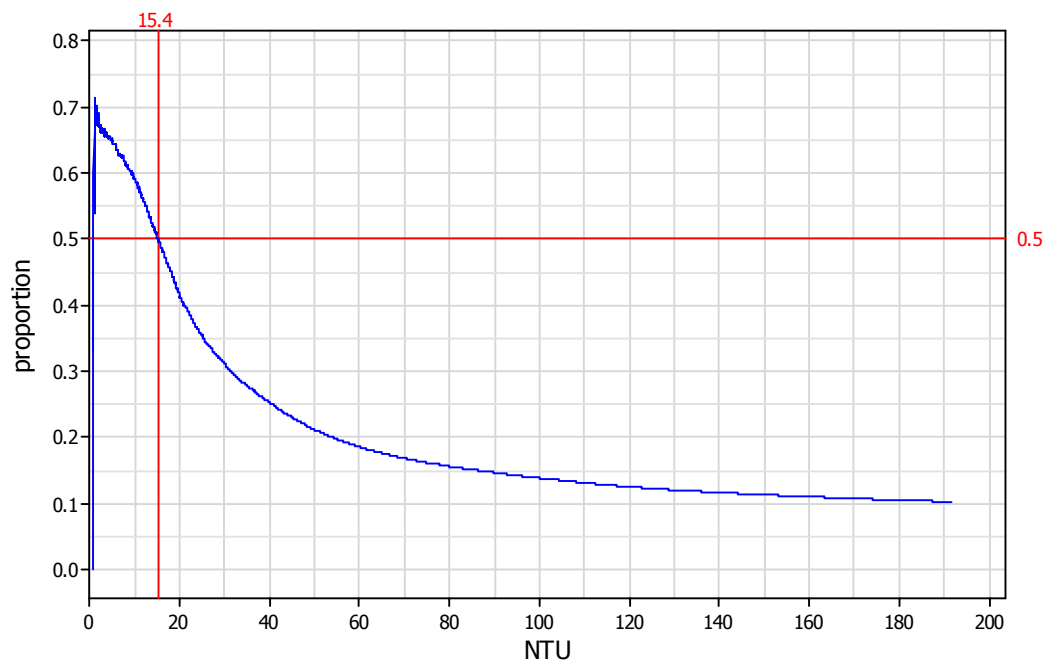
Figure 12. Plot of (empirical) probability that 15% light requirement being met at site 2006 under 'worst-case' conditions as a function of *NTU* limit.

Significance of the results

The analysis of the 'worst-case' scenario clearly indicates that without intervention, there will be periods during which the minimum light requirement will not be met. The issue then becomes one of managing the *NTU* during the worst-case two week period (or some other suitably chosen interval). In order to meet the light requirement at site 2006 of 15% surface irradiance at 3m depth for at least 50% of the time during the 'worst' periods of the dredging campaign, the *NTU* will need to be kept below 15 units.

3. REFERENCES

Environmetrics Australia (2007) An Examination of Regression Options for TSS and NTU. Report to Port of Melbourne Corporation, February 2007.

Baker, E.T. and .Lavelle, J.W. (1984) The effect of particle size on the light attenuation coefficient of natural suspensions. *Journal of Geophysical Research,* **89(C12),** 8197-8204.

Longmore, A. (2006) Channel Deepening project: Further study of the relationships between suspended solids, turbidity and light attenuation. Dept. of Primary Industries, Queenscliff, Victoria.

APPENDIX A: RELATIONSHIP BETWEEN TSS AND Kd

This appendix provides details on the regression modelling used to establish parameter estimates for equation 3 in the main text of this report (reproduced below as equation A.1).

$$Kd_j = \gamma_0 + \gamma_1 \left(TSS_j \right) + \xi_j \qquad (A.1)$$

Kd is the light attenuation coefficient $\left(m^{-1} \right)$ and *TSS* is the suspended sediment concentration (mg/L); γ_0 and γ_1 are the true (unknown) regression parameters; and ξ_j is a random error component associated with the jth observation and which is assumed to be normally distributed about a zero mean and having variance σ_ξ^2.

A-1.   Regression Modelling

Given data on *TSS* and *Kd* the parameters in Equation A.1 can be estimated using ordinary least-squares. Two data sets were made available by the Port of Melbourne Corporation for this purpose. The first of these was laboratory data used by Longmore (2006). Figure A.1 shows the relationship between *Kd* and *TSS* for different sediment types in the southern portion of Port Phillip Bay.
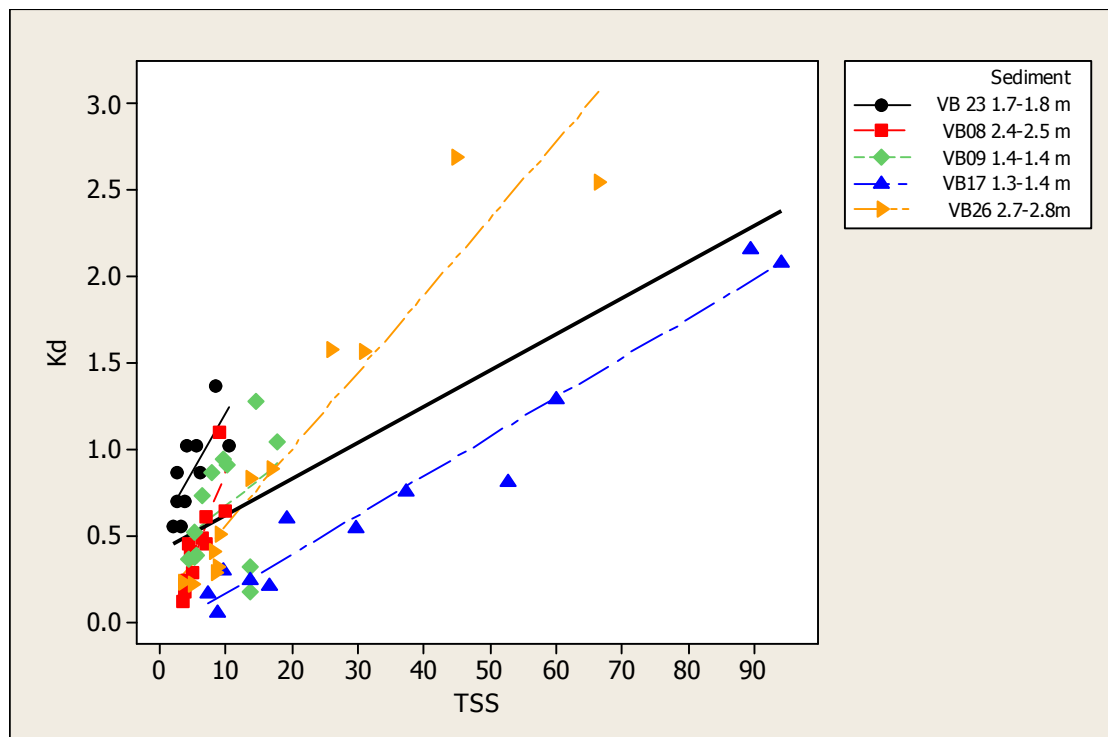

Figure A.1. Relationship between *Kd* and *TSS* for different sediment types in southern region of the Bay. Black solid line is overall regression fit (data taken from Longmore, 2006).

These data were considered to be useful for establishing the relationship between *Kd* and *TSS* under relatively high suspended sediment loads (as expected during dredging), but were not considered representative of background conditions where the predominant factors contributing to the ambient or background *Kd* is CDOM, algal pigments, and organic particulates. A number of previous studies have investigated background *Kd* for the waters of Port Phillip Bay. Data from two sources (PIRViC and SKM) for the southern regions of Port Phillip Bay was supplied to Environmetrics Australia by the Port of Melbourne Corporation. A graphical summary of the background light attenuation coefficients at Blairgowrie, Cameron's Bight, and Rye is shown in Figure A.2.
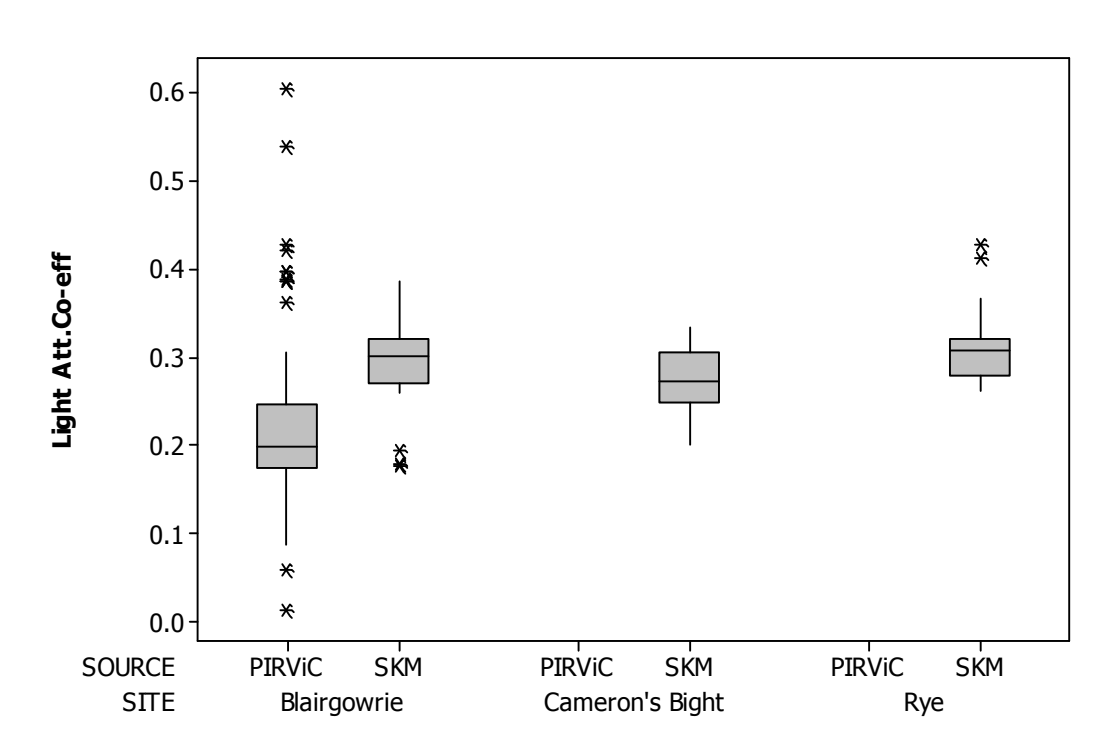
Figure A.2. Box-plots of background *Kd* values at three sites.

A numerical summary of the data in Figure A.1 broken down by site and source appears below.

```
Blairgowrie

Variable          SOURCE    N   N*     Mean   SE Mean     StDev   Minimum       Q1    Median       Q3   Maximum
Light Att.Co-eff  PIRViC  157    0  0.21487   0.00609   0.07633   0.01356  0.17540   0.19923  0.24716   0.60332
                  SKM      25    0   0.2902    0.0102    0.0512    0.1772   0.2705    0.3003   0.3200    0.3859


Cameron's Bight

Variable          SOURCE  N  N*    Mean   SE Mean    StDev   Minimum      Q1   Median      Q3   Maximum
Light Att.Co-eff  SKM     8   0  0.2718    0.0144   0.0406    0.2015  0.2493   0.2727  0.3055    0.3335
```

Rye

```
Variable                SOURCE   N  N*     Mean  SE Mean    StDev  Minimum       Q1   Median       Q3  Maximum
Light Att.Co-eff  SKM    22   0  0.31110  0.00927  0.04346  0.26147  0.27841  0.30674  0.32148  0.42751
```

Figure A.2 and the descriptive statistics suggest that there is reasonably good agreement among the sites although the PIRViC data at Blairgowrie has a higher mean and variance. Reasons for this could be explored, although for the purpose of the current exercise, this was not considered to be warranted. A numerical summary of the SKM data grouped (over all sites) is as follows.

Table 2. Summary of background *Kd* data for Blairgowrie, Cameron's Bight, and Rye (SKM data).

```
Variable            N  N*     Mean  SE Mean    StDev  Minimum       Q1   Median       Q3  Maximum
Light Att.Co-eff   55   0  0.29587  0.00648  0.04803  0.17725  0.27151  0.29806  0.31853  0.42751
```

The overall mean attenuation coefficient based on the SKM data is 0.29587. It is interesting to compare this with the intercepts (γ_0 in Equation A.1) that were estimated using the Longmore (2006) data (Table A.2).

Table A.3. Estimated intercepts for Equation A.1 at selected sites.

Site	$\hat{\gamma}_0$	Std. error
Yarra	0.3011	0.1764
Williamstown	0.2146	0.1298
PMCh	0.3426	0.1267
Southern	0.41267	0.06780

The average of the 4 $\hat{\gamma}_0$ values in Table A.2 is 0.3177 which accords with the 0.2 to 0.35 range reported by Jupp et al. (1996). The estimated intercept of 0.41267 for the Southern region (Table A.2) is about 40% higher than the average of the SKM data (Table A.1) and is possibly due to the previously noted inconsistencies between the *Kd* values derived from laboratory and field experiments. For this report, an estimate of the overall background *Kd* is based on the results of Table A.1 rather than the individual estimates given in Table A.2. Thus $\hat{\gamma}_0$ is taken to be 0.29587 with a

standard error of 0.04803. γ_1 of Equation A.1 is then estimated subject to the constraint that $\hat{\gamma}_0 = 0.29587$. The computational details are explained in the next section.

A-2.   Parameter Estimation

Let $\begin{bmatrix} \hat{\gamma}_0 & \hat{\gamma}_1 \end{bmatrix}^T$ be the (2 x 1) vector of estimated parameters in Equation A.1 with corresponding covariance matrix Σ obtained by ordinary least squares regression using the Longmore (2006) experimental data. The structure of the estimated Σ is as follows:

$$\hat{\Sigma} = \begin{pmatrix} \hat{\sigma}_{00} & \hat{\sigma}_{01} \\ \hat{\sigma}_{01} & \hat{\sigma}_{11} \end{pmatrix} \tag{A.2}$$

where $Var\begin{bmatrix} \hat{\gamma}_i \end{bmatrix} = \sigma_{ii}$ and $Covar\begin{bmatrix} \hat{\gamma}_i & \hat{\gamma}_j \end{bmatrix} = \sigma_{ij}$. Furthermore, the *correlation* between the parameter estimates is:

$$\hat{\rho}_{01} = \frac{\hat{\sigma}_{01}}{\sqrt{\hat{\sigma}_{00}} \sqrt{\hat{\sigma}_{11}}} \tag{A.3}$$

For reasons given above, $\hat{\gamma}_0$ of Equation A.1 is replaced with an estimate obtained from an independent source (SKM). Denote the SKM estimate as $\tilde{\gamma}_0$ and the variance of this estimate by $\tilde{\sigma}_{00}$. The variance $\tilde{\sigma}_{00}$ can replace $\hat{\sigma}_{00}$ in Equation A.2. To preserve the correlation given by equation A.3, a revised estimate of the covariance $\hat{\sigma}_{01}$ needs to be provided. The revised estimate $\tilde{\sigma}_{01}$ is given by Equation A.4.

$$\tilde{\sigma}_{01} = \hat{\rho}_{01} \sqrt{\tilde{\sigma}_{00}} \sqrt{\hat{\sigma}_{11}} \tag{A.3}$$

Thus, the revised covariance matrix, $\tilde{\Sigma}$ becomes

$$\hat{\Sigma} = \begin{pmatrix} \tilde{\sigma}_{00} & \tilde{\sigma}_{01} \\ \tilde{\sigma}_{01} & \hat{\sigma}_{11} \end{pmatrix} \tag{A.5}$$

A-3.   Results

Results of the overall regression modelling using Longmore's (2006) data are given in Box A.1.

Box A.1. Regression analysis for *Kd* and *TSS* (refer Equation A.1) using the original Longmore (2006) data.

```
The regression equation is
Kd = 0.413 + 0.0209 TSS


Predictor       Coef    SE Coef     T       P
Constant     0.41267    0.06780   6.09   0.000
TSS          0.020929  0.002670   7.84   0.000


S = 0.407283   R-Sq = 52.3%   R-Sq(adj) = 51.5%


Analysis of Variance

Source          DF       SS       MS       F       P
Regression       1    10.191   10.191   61.44   0.000
Residual Error  56     9.289    0.166
Total           57    19.480
```

The covariance matrix of the estimated parameters in Box A.1 is:

$$\hat{\Sigma} = \begin{pmatrix} 0.0045966 & \text{-}0.0001113 \\ \text{-}0.0001113 & 0.0000071 \end{pmatrix}$$

and by Equation A.3, the correlation coefficient $\hat{\rho}_{01} = $ -0.616.

As detailed the previous sections, we wish to constrain the intercept ($\hat{\gamma}_0$) in Equation A.1 to the average background attenuation coefficient – call this $\tilde{\gamma}_0$. This gives a revised estimate of $\hat{\gamma}_1$ of 0.023757 (cf. previously estimated 0.020929 in Box A.1).

APPENDIX B: VARIANCE OF PREDICTED TSS and Kd

Figures 1 and 2 as well as equations 1 and 2 in the main text illustrate the process by which the probabilistic analysis of benthic light conditions was undertaken. Figure 2 shows the various sources of uncertainty and a pivotal component of the modelling is the accurate representation of these elements. The simulation procedure identified in Figure 2 commences with the generation of random *NTU* data from an appropriate probability model. These are converted into predicted *TSS* values using the regression model of equation 1. The predicted *TSS* (and its uncertainty) become inputs to the next regression model, equation 3. This appendix provides the necessary expressions for the variance associated with the predicted *TSS* and *Kd* values. Although equation 1 sets $\beta_0 = 0$ (i.e. regression through the origin), the following results apply to both zero and non-zero intercepts.

Now, under the assumptions of equation 1, a *predicted* value for an *individual TSS* (call it $\widehat{TSS}_0$) corresponding to a single turbidity reading (denoted x_0) follows a normal distribution with the following mean and variance:

$$E\left[\widehat{TSS}_0\right] = \underline{a}\hat{\beta} \tag{B.1}$$

$$\text{var}\left[\widehat{TSS}_0\right] = \sigma_\varepsilon^2\left[1 + \underline{a}\left(X^T X\right)^{-1}\underline{a}^T\right] \tag{B.2}$$

where $\underline{a} = \begin{bmatrix} 1 & x_0 \end{bmatrix}$; $\hat{\beta}^T = \begin{bmatrix} \hat{\beta}_0 & \hat{\beta}_1 \end{bmatrix}$; and $X = \begin{bmatrix} \underline{1} & \underline{x} \end{bmatrix}$ where $\underline{1}$ is a column of ones and $\underline{x}$ is a column containing the original *NTU* readings used to estimate the regression parameters of Equation 1.

Likewise, a *predicted* value for an individual *Kd* (call it $\widehat{Kd}_0$) corresponding to a single *TSS* value (denoted w_0) will be also normally distributed with mean and variance:

$$E\left[\widehat{Kd}_0\right] = \underline{b}\hat{\gamma} \tag{B.3}$$

$$\text{var}\left[\widehat{Kd}_0\right] = \sigma_\xi^2\left[1 + \underline{b}\left(W^T W\right)^{-1}\underline{b}^T\right] \tag{B.4}$$

where $\underline{b} = \begin{bmatrix} 1 & w_0 \end{bmatrix}$; $\hat{\gamma}^T = \begin{bmatrix} \hat{\gamma}_0 & \hat{\gamma}_1 \end{bmatrix}$; and $W = \begin{bmatrix} \underline{1} & \underline{w} \end{bmatrix}$ where $\underline{1}$ is a column of ones and $\underline{w}$ is a column containing the original *TSS* readings used to estimate the regression parameters of Equation 3.